# Liquid Sampling–Atmospheric Pressure Glow Discharge as a Secondary Excitation Source for Laser Ablation-Generated Aerosols: Parametric Dependence and Robustness to Particle Loading

**Benjamin T. Manard,[a,b] Stefanie Konegger-Kappel,[a] Jhanis J. Gonzalez,[b] Jose Chirinos,[b] Meirong Dong,[b] Xianglei Mao,[b] R. Kenneth Marcus,[a,*] Richard E. Russo[b]**

[a] *Clemson University, Department of Chemistry, Biosystems Research Complex, 51 New Cherry Street, Clemson, SC 29634 USA*
[b] *University of California–Berkeley, Lawrence Berkeley National Laboratory, 1 Cyclotron Road, Berkeley, CA 94720 USA*

**Liquid sampling–atmospheric pressure glow discharge (LS-APGD) microplasma is being developed as a secondary vaporization–excitation source for the optical emission analysis of laser ablation (LA)-generated particle populations. The practicalities of this coupling are evaluated by determining the influence of source parameters on the emission response and the plasma's robustness upon LA introduction of easily ionized elements (EIEs). The influence of discharge current (45–70 mA), LA carrier gas flow rate (0.1–0.8 L $min^{-1}$), and electrode separation distance (0.5–3.5 mm) was studied by measuring Cu emission lines after ablation of a brass sample. Best emission responses were observed for high-discharge currents, low He carrier gas flow rates, and relatively small ($<$1.5 mm) electrode gaps. Plasma robustness and spectroscopic matrix effects were studied by monitoring Mg(II) : Mg(I) intensity ratios and $N_2$-derived plasma rotational temperatures after the ablation of Sr- and Ca-containing pellets. Plasma robustness investigations showed that the plasma is not appreciably affected by the particle loadings, with the microplasma being slightly more ionizing in the case of Ca introduction. In neither case did the concentration of the concomitant element change the robustness values, implying a high level of robustness. Introduction of the LA particles results in slight increases in the rotational temperatures ($\sim$10% relative), with Ca-containing particles having a greater effect than Sr-containing particles. The observed variation of 9% in the plasma rotational temperature is in the same order of magnitude as the short-term reproducibility determined by the proposed LA-LS-APGD system. The determined rotational temperatures ranged from 1047 to 1212 K upon introducing various amounts of Ca and Sr. The relative immunity to LA particle-induced matrix effects is attributed to the relatively long residence times and high power densities ($>$10 W $mm^{-3}$) of the LS-APGD microplasma.**

Index Headings: **Liquid sampling–atmospheric pressure glow discharge; LS-APGD; Laser ablation; Optical emission spectroscopy; Excitation conditions; Robustness; Particle loading.**

## INTRODUCTION

The development of analytical chemistry instrumentation in the fields of chemical separation, electrochemistry, and mass and optical spectrometric analyses has progressed considerably over the last decade in terms of miniaturization.[1,2] However, relatively little progress has been realized in the miniaturization of atomic spectroscopy instrumentation. The availability of miniaturized instrumentation in general is important for several reasons, but it is of crucial importance for prompt field analyses. Field-deployable instruments for elemental, isotopic, or molecular characterizations of environmental samples would allow for, e.g., prompt environmental contamination and nuclear mishap screenings and forensic analyses. Rapid assessment of such samples provides baseline information for materials to be collected for a more thorough analysis in the laboratory—a form of triage. One of the greatest challenges to "field" analyses is the need for methods to be highly robust in terms of the diversity of potential sample matrices. This robustness is not only required of the measurement method but also for the chemical manipulations of diverse materials, making them amenable to analysis. The ability to analyze samples without laborious sample preparation procedures (i.e., digestion) has been advanced with the implementation of laser ablation (LA) methods,[3–5] allowing for the direct sampling of solids.

In laser ablation, a short-pulsed (femtoseconds to nanoseconds), high-power (Watts) laser beam is typically focused onto a solid sample, resulting in melting–vaporization of the sample surface.[3,6] Generally, after the ejection of ablated material, there are two means of determining the sample's elemental composition: (1) direct analysis of the laser-induced plume at the ablation site by optical emission spectroscopy (OES), which is commonly referred to as laser-induced breakdown spectroscopy (LIBS); and (2) analysis by OES or mass spectrometry (MS) after transportation of the particulate population to a secondary excitation–ionization source, which is in most cases an inductively coupled plasma (ICP).[3,4,7,8] Because of its small footprint, compared to ICP-OES-MS, and the fact that only minimal or even no sample preparation is needed, LIBS is highly appreciated in case of field-deployable instruments. The use of LIBS has expanded to planetary[9] and underwater elemental[10,11] analyses. However, increased sensitivity is realized when the LA-generated aerosol is subject to secondary ionization–excitation. Typically, secondary excitation sources such as the ICP, exhibit higher power densities ($\sim$1 W $mm^{-3}$) and longer analyte plasma residence times ($\sim$5 ms) than the actual laser-induced plasma, commonly yielding higher sensitivity for elemental analysis.[4] In the context of miniaturized–transportable systems, the ICP has a relatively large footprint, high operating costs due to high gas

Received 6 May 2014; accepted 8 July 2014.
* Author to whom correspondence should be sent. E-mail: marcusr@clemson.edu.
DOI: 10.1366/14-07585


0003-7028/15/6901-0058/0

**TABLE I. Pellet compositions and thermodynamic properties of concomitant metals.**

| No. | % $CaCO_3$ | % $SrCO_3$ | Properties of concomitants | Ca | Sr |
|---|---|---|---|---|---|
| 1 | 1.2 | 0.16 | First ionization potential (eV) | 6.1 | 5.7 |
| 2 | 2.5 | 0.34 | Second ionization potential (eV) | 11.9 | 11.0 |
| 3 | 5 | 0.84 | Heat of vaporization (kJ $mol^{-1}$) | 154.7 | 136.9 |
| 4 | 10 | 1.7 | Boiling point (K) | 1484 | 1382 |
| 5 | 15 | 3.4 | Metal-oxide bond energy (kJ $mol^{-1}$) | 464 | 454 |
| 6 | 20 | 6.7 | | | |
| 7 | 22.5 | 10.1 | | | |
| 8 | 25 | 13.9 | | | |
| 9 | n/a | 15.1 | | | |
| 10 | n/a | 16.8 | | | |

[a]n/a = not applicable.

consumption ($\sim$15 L $min^{-1}$), and high power requirements (1–1.5 kW). While the ICP is the most commonly used secondary excitation source,[5,8,12] its relatively large volume (i.e., $\sim$125 $mm^3$) effectively leads to a "dilution" of the LA-generated aerosol. Thus, it would seem that the coupling of LA with a miniaturized source, having the basic characteristics to allow field deployment and having a much smaller plasma volume might find particular utility.

The usefulness of coupling LA with small-volume discharges has been addressed in some part. For example, an LA spark-induced breakdown spectroscopy (LA-SIBS) was demonstrated by Li et al.[13] Studies revealed improved emission and signal-to-noise ratios (S/Ns) compared to conventional LIBS without the need for analyte transport. However, high voltages ($\sim$10 kV) were required for the discharge to be sustained, which could be disadvantageous in terms of instrument portability.[13] Glow discharge (GD) plasmas using a hollow-cathode geometry have also been employed as secondary excitation sources for LA-generated aerosol dating back to Iida.[14] More recently, Tereszchuk et al.[15] demonstrated the use of a synchronized, pulsed direct current (DC) GD as a secondary excitation source for copper samples with OES detection. Studies revealed an up to 75-fold signal enhancement compared to a traditional LIBS setup.[15] While interesting from the point of view of performance, and deserving of further evaluation, use of in vacua discharges is again problematic in terms of potential portability. The development of GD plasmas initiated at the surface of liquids as excitation–ionization sources in atomic spectroscopy has been demonstrated over the last decade, as highlighted by several reviews dedicated to this area.[16–20] Low power, compactness, and experimental simplicity result in the attractiveness of such devices in miniaturized elemental analysis instrumentation.

Marcus and coworkers have recently used the liquid sampling atmospheric pressure GD (LS-APGD) microplasma as a secondary excitation–ionization source for LA-produced particles.[21–23] The plasma, operating at powers of $<$50 W, is formed between an electrolytic solution acting as one electrode and a counter electrode.[23–25] The LS-APGD has a small plasma volume ($<$1 $mm^3$), yielding power densities in the 10s W $mm^{-3}$ range versus $\sim$0.1 $mm^{-3}$ for the ICP, while also having dramatically lower support gas flow rates ($<$1 L $min^{-1}$). As demonstrated in the present work, the entirety of the source hardware, including laser, can be fit onto a 0.09 $m^2$ optical platform.

Indeed, these basic characteristics bode well in the context of miniaturized, field-deployable instrumentation. The ability to perform rapid analysis without sample digestion (due to laser ablation) and high level of robustness of the microplasma imply that experiments can indeed be performed outside of the laboratory. Of course, different from LIBS, the need for a carrier gas, the plasma sustaining liquid, and the power supply would be added overhead.

The plasma characteristics (i.e., plasma temperatures, electron number density, and robustness) have been investigated recently in hopes of a better understanding of the LS-APGD's potential as an excitation–ionization source for liquid samples.[23,26] While the plasma excitation temperature ($\sim$2600 K) may not be as high as that of a typical ICP (typically 7000–10 000 K), the electron number density ($3 \times 10^{15}$ $cm^{-3}$) is on the same order of magnitude. Rotational temperatures determined through OH and $N_2$ band emission are $\sim$1000 K.[23] While such values seem to be low in terms of vaporization capacity, the device has been shown to be effective as a secondary excitation–ionization source for particles generated by both nanosecond and femtosecond laser ablation.

The aim of this work is determining the influence of microplasma operating parameters on the LS-APGD's emission response and the investigation of plasma robustness after solid sampling by means of laser ablation. While effort has been put into the investigation of these plasma characteristics in the case of liquid sampling, a detailed study of how aerosol particles effect the plasma environment has not yet been approached. The knowledge and understanding of such plasma characteristics are of crucial importance for further method developments and the full assessment of the source's utility in atomic spectroscopy, using both liquid and solid sampling. LA-LS-APGD operating parameters including GD current, carrier gas flow rate, and distance between the electrodes were evaluated here by ablating a brass sample and measuring the resultant Cu(I) responses. Plasma robustness and spectroscopic matrix effects were assessed by determining Mg(II) : Mg(I) emission line ratios and plasma rotational temperatures after introducing an LA-generated aerosol containing easily ionized elements (i.e., Ca and Sr) into the plasma. It is believed that the high plasma power density allows for the effective digestion of LA-generated particles as any effects are hardly outside of the experimental variability.

## EXPERIMENTAL

**Materials.** Test pellets were prepared in-house at Lawrence Berkeley National Laboratory by mixing paraffin-binder (3436 SPEX SamplePrep, Metuchen, NJ) with magnesium carbonate ($MgCO_3$), strontium carbonate ($SrCO_3$), and calcium carbonate ($CaCO_3$) powders. $SrCO_3$ and $CaCO_3$ (Sigma Aldrich, St. Louis, MO) amounts were varied from $\sim$0.1 to $\sim$17% (w/w) and from $\sim$1 to 25% (w/w), respectively (see Table I), while the $MgCO_3$ (Sigma Aldrich) amount was kept constant (3.43% (w/w)) in all

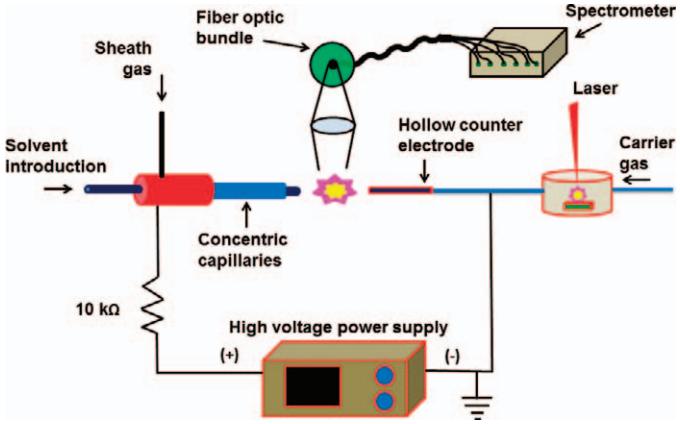


FIG. 1. LS-APGD-OES source components for the analysis of LA-generated particle populations.

pellets. Upon mixing, pressing was performed with a 3630 X-Press (SPEX SamplePrep) under 25 tons with a hold time of 2 min and release time of 1 min. While not within the scope of the present study, response curves measured by means of the LA-LS-APGD system showed correlation coefficients ($R^2$) greater than 0.90 for both Sr- and Ca-containing pellets across these concentration ranges. A stock brass sample was used as a representative homogeneous metal for the parametric evaluation.

## LASER-ABLATION LIQUID-SAMPLING ATMOSPHERIC PRESSURE GLOW DISCHARGE OPTICAL EMISSION SPECTROSCOPY (LA-LS-APGD-OES) SYSTEM

**Liquid Sampling–Atmospheric Pressure Glow Discharge.** The base LS-APGD source design used in this study was slightly modified to allow for the introduction of LA-generated particles by using a hollow counter electrode as seen in Fig. 1 and described previously.[22,23] The first difference from the earlier work is in the construction of the source, where the footprint of the LS-APGD system was decreased by more than a factor of 2. This was affected through more judicious choices in system components. The microplasma was sustained between two electrodes: an electrode containing an electrolytic solution and a hollow metallic counter electrode. (In principle, two "solid electrodes" could serve to sustain the plasma much like a conventional DC arc, but this is beyond the scope of this work.) The electrolytic solution (1 mol $L^{-1}$ nitric acid [$HNO_3$], OmniTrace Ultra, EMD Millipore, Billerica, MA) flowing by means of a syringe pump (model NE-1000 Multi-Phaser, New Era Pump Systems Inc., Farmingdale, NY) in a fused silica capillary (i.e., 360 μm outer diameter (o.d.), 100 μm inner diameter (i.d.), Idex Health and Science, Oak Harbor, WA) served as the anode, while the counter electrode served as the cathode. The silica capillary was encircled within a metal capillary (nickel, 0.16 cm o.d., 0.06 cm i.d.), with the He sheath gas flowing in the intercapillary gap for plasma stability. A power supply (0–100 mA, 2 kV, Glassman High Voltage Inc., High Bridge, NJ) was used, with a 10 kΩ, 225 W ballast resistor (Ohmite, Arlington Heights, IL) placed in-line before connection with the anode. A hollow tube (nickel, 0.3 cm o.d., 0.1 cm i.d.) was used as the counter electrode to allow for the transport of the LA-generated particles from the ablation chamber to the microplasma.

A more substantial change in the present source dealt with the shielding of the counter electrode. Different from the previous studies is the use of a glass sleeve on the outside of the counter electrode to restrict the available electrode surface area to 1 mm from the electrode tip. Without this restriction, a "normal" GD results, meaning that increases in current simply cause the spread of the current. Thus, the current density, and the voltage required to maintain it are constant. Restriction of the counter electrode surface area creates a situation where increased current leads to higher current densities and higher voltages, an "abnormal " GD. For this particular system, the operating voltage is invariate with voltage (averaging ~330 V) without the use of the glass sleeve, but varies virtually linearly from 380 to 440 V across the current range of 50–65 mA. The instrument operation parameters are given in Table II.

TABLE II. Instrument components and operational parameters.

| | IR ablation | UV ablation |
|---|---|---|
| LA J200 system | | |
| Wavelength (nm) | 1064 | 213 |
| Pulse width (ns) | 5 | 3 |
| Energy (mJ) | 50 | 5 |
| Repetition rate (Hz) | 10 | 10 |
| No. of shots | 150 | 150 |
| No. of replicates | 4 | 4 |
| He carrier gas flow rate (L $min^{-1}$) | 0.1–0.8 | 0.1–0.8 |
| LS-APGD microplasma | | |
| Sheath gas flow rate (L $min^{-1}$) | 0.2 | 0.2 |
| Electrolytic solution [5% $HNO_3$ (v/v)/μL $min^{-1}$] | 200 | 200 |
| Electrode separation distance (mm) | 0.5–3.5 | 0.5–3.5 |
| GD current (mA) | 45–70 | 45–70 |
| Aurora optical emission spectrometer | | |
| Integration time (ms) | 1.05 | |
| Spectral resolution (nm) | 0.05–0.12 (190–1040) | |
| Spectrometer | Six-channel CCD (Aurora) | |
| Detector | 2048 pixel CCD for each channel | |

**Laser Ablation.** Laser ablation was accomplished by means of a commercial nanosecond Laser Ablation–LIBS system (J200, Applied Spectra, Inc., Fremont, CA). The system was operated at the fundamental infrared (IR) wavelength (1064 nm) and in the ultraviolet (UV) region (213 nm). The previous works only involved IR irradiation.[22] Instrumental parameters are given in Table II. The LA-generated aerosol was transported to the LS-APGD using He as a carrier gas. A transport tube consisting of 6.35 mm (0.25 in) i.d. Tygon tubing (Saint-Gobain, Courbevoie, France) was used to connect the ablation chamber to the hollow counter electrode.

**Optical Emission Spectrometer.** Emission from the LS-APGD microplasma was collected by a fused silica biconvex lens (35 mm focal length, 25.4 mm diameter, Thorlabs Inc., Newton, NJ). A charge-coupled device (CCD)–based spectrometer (Applied Spectra, Inc.) was used for all OES measurements. The spectrometer was equipped with six channels; each channel used a 2048 pixel CCD detector, enabling the acquisition of composite spectra simultaneously across a wavelength range of 190–1040 nm. Spectra were generated for each experi-

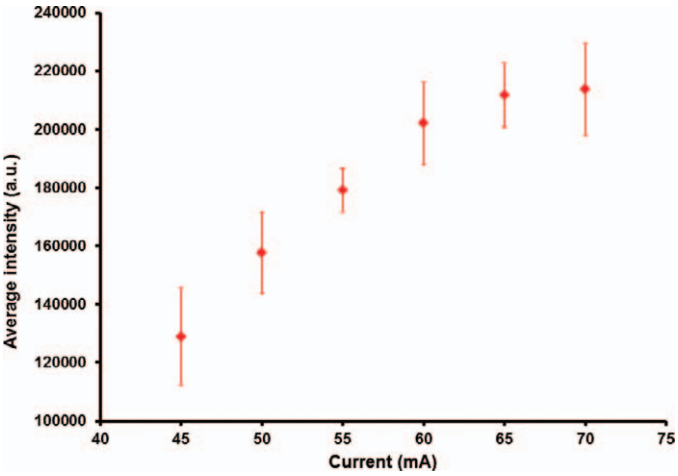


FIG. 2. Cu(I) 327.4 nm emission response as a function of LS-APGD discharge current. All other parameters constant: interelectrode separation = 1.0 mm, He sheath gas flow rate = 0.2 L $min^{-1}$, solution flow rate = 200 μL $min^{-1}$ (5% $HNO_3$), He carrier gas flow rate = 0.2 L $min^{-1}$, 1064 nm laser energy = 50 mJ, repetition rate = 10 Hz, target = brass alloy.

mental condition by co-adding the emission responses for 150 laser shots in a single location. Data processing (signal accumulation and background subtraction) was performed using the Aurora software (Applied Spectra, Inc.), and Excel (Microsoft, Redmond, WA) was used for further data evaluations. Optical response data reported here are given as the average of triplicate repetitions (under each condition), with ±1 SD variance.

**Optimization of Laser-Ablation Liquid Sampling–Atmospheric Pressure Glow Discharge Optical Emission Spectroscopy System.** Optimization of LA-LS-APGD parameters was accomplished by monitoring Cu(I) emission lines (i.e., 324.7 nm ($E_{exc}$ = 3.81 eV), 327.4 nm ($E_{exc}$ = 3.78 eV), 510.5 nm ($E_{exc}$ = 6.19 eV), and 521.8 nm ($E_{exc}$ = 3.81 eV)) during the course of ablation of a brass sample using a laser wavelength of 1064 nm. Zn, also in the brass sample, provided the opportunity to study alternative element–transition energies, specifically the Zn(I) 472.1 and 480.9 nm ($E_{exc}$ = 6.65 eV) transitions. Studies currently underway using solution sample introduction are looking to the responses of a wide variety of elements and transitions to changes in discharge conditions. A previous evaluation of the LA-LS-APGD system looked at the roles of discharge current and carrier gas flow rate.[22] However, as a slightly modified (specifically the restricted counter electrode surface area) discharge system and LA apparatus were used in this study, the roles of discharge current, He carrier gas flow rate, and electrode separation distance were readdressed. These parameters were evaluated for both IR and UV ablation wavelengths. Once the parametric dependences were evaluated, the reproducibility of the entire LA-LS-APGD-OES system was evaluated using the homogeneous brass alloy and a compacted paraffin sample containing 3.38% (w/w) $SrCO_3$. In the first case, a laser wavelength of 1064 nm was applied, with 213 nm used for the compacted sample as a different LA apparatus was used. In both instances, spot-to-spot variations (150 shots per spot) in the analyte (Cu and Sr) responses showed variability of ~8% relative standard deviation (RSD). Thus, it was concluded that the reproducibility of the laser sampling and the stability of the plasma source were of a sufficient level to look at samples having different compositions to study potential matrix effects.

## RESULTS AND DISCUSSION

**Influence of Glow Discharge Current on Emission Response.** The processes of converting brass particulates to excited state Cu atoms that are observed through their optical emission are kinetically driven. LA particles must be subjected to sufficient heat to completely vaporize them, after which collisions with plasma electrons or He metastable atoms (i.e., Penning collisions) affect the excited state populations of the atomic vapor.[26] Discharge current would be expected to play a role in the gas kinetic temperature of the plasma as well as in the rate of excited state-populating collisions. To a first approximation, higher discharge currents, and correspondingly higher power densities, would be expected to yield higher plasma temperatures (e.g., better vaporization), while also providing higher electron–atom collision rates. Recent studies by Russo and coworkers show small (<10% relative) increases in rotational temperatures ($T_{rot}$) and excitation temperatures ($T_{exc}$) values with increasing current, while electron number densities are virtually invariant with changes in discharge current over the range 45–65 mA.[23] Thus, it would be expected that optimum atomic emission response should be found at high discharge currents.

The responses of Cu(I) 327.4 nm emission intensity are proportional to increases in discharge current over the range 45–65 mA for particles generated under 1064 and 213 nm, with the response plateauing beyond this point, as depicted in Fig. 2. The response increases by approximately two times over this current range for the case of 1064 nm ablation. Each of the monitored Cu(I) and Zn(I) transitions followed the same general trend. Indeed, the lack of any differences suggests that (1) there are no appreciable changes in excitation conditions (e.g., temperatures) and (2) self-absorption of resonant Cu(I) lines was insignificant (as differences would be quite apparent). The proportional increase found here is virtually the same as observed in previous LA-LS-APGD works using 1064 nm irradiation.[22] In both instances, very little Cu(I) response was observed for discharge currents of <45 mA, which is attributed to insufficient plasma (power) density to affect efficient particle vaporization. The lack of increased yields at higher currents (>70 mA) might suggest that the cumulative vaporization–excitation processes are sufficient to deal with the introduced particle population, as further increases do not increase the number of emitting atoms. In addition, beyond ~70 mA, higher currents lead to counter electrode overheating and damage (remembering that it serves as the cathode and thus is subjected to ion bombardment). Electrode overheating results in increased variability in the Cu(I) emission data, without the benefit of greater photon fluxes.

**Influence of Electrode Separation Distance and Laser Ablation Carrier Gas Flow Rate on Emission Response.** While the above-cited temperature characteristics reflect the ability of the plasma to affect the work

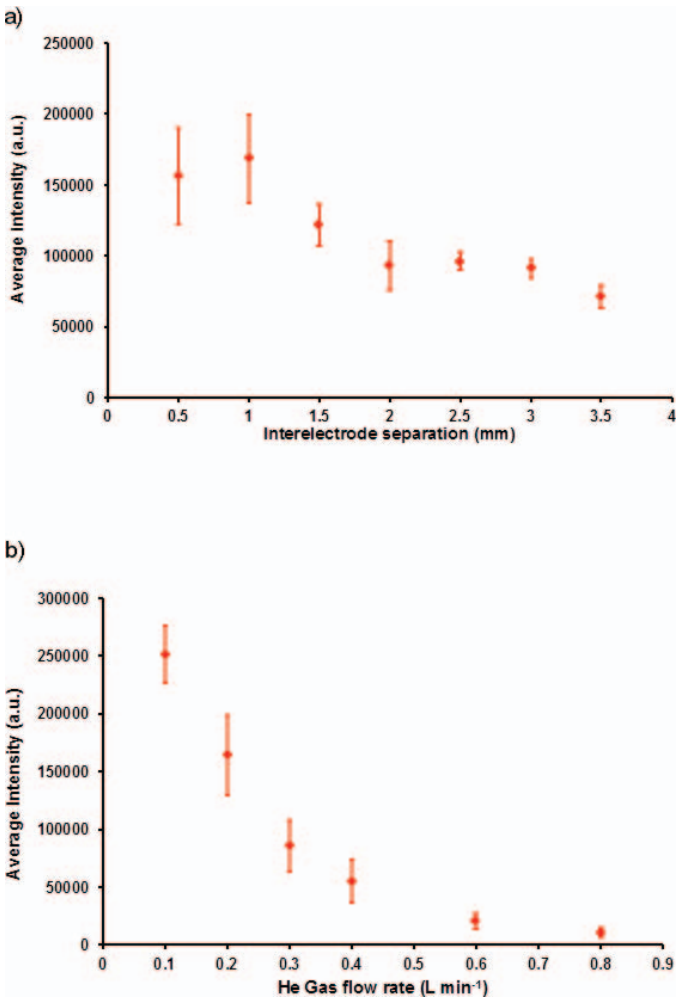


FIG. 3. Cu(I) 327.4 nm emission response as a function of (**a**) interelectrode separation distance for a carrier gas flow rate of 0.2 L $min^{-1}$ and (**b**) He carrier gas flow rate for an interelectrode separation of 1.0 mm. All other parameters constant: He sheath gas flow rate = 0.2 L $min^{-1}$, solution flow rate 200 μL $min^{-1}$ (5% $HNO_3$), discharge current = 60 mA, 1064 nm laser energy = 50 mJ, repetition rate = 10 Hz, target = brass alloy.

in converting LA particulates into emitting atoms, the residence time of those species in the active microplasma environment is expected to be equally important in the analytical context. In general, emission responses should be improved by extended analyte residence times in an excitation source so long as gas phase reactions do not result in the loss of the target atoms (e.g., reactions that cause formation of metal oxides). Parameters assumed to affect residence times in the LS-APGD are the interelectrode separation and the particle flow rate into the microplasma. While increasing electrode separation would increase the residence time, decreases in plasma power density would also result; so, there may certainly be trade-offs in terms of available energy and exposure time. In contrast, particles are carried into, and swept through, the plasma volume by means of the LA carrier gas flow. As in the case of ICP sources, it would be expected that higher carrier gas flow rates would decrease residence times.[27,28] An additional consideration that is not explicitly addressed here is the fact that there is an opposing gas flow to the particle carrier gas, the sheath–cooling gas from the liquid electrode, which would contribute to the overall gas dynamics and microplasma residence times.

As depicted in the Cu(I) responses plotted in Fig. 3a, there is indeed a trade-off seen between the interelectrode separation in terms of the plasma density and the residence time for a fixed carrier gas flow rate of 0.1 mL $min^{-1}$. Previous work indicated that there is a slight positive correlation between the electrode distances and $T_{rot}$ and $T_{exc}$, with a slight negative correlation with electron number density ($n_e$) values for the LS-APGD.[23] A very simple gas velocity calculation based on the carrier gas flow rate suggests transit times ranging from 0.2 to 1.6 ms across this range of separation distances. (In reality, the counter-propagating sheath gas from the liquid electrode will contribute to the overall particle paths and likely increased residence times.) The maximum in Cu(I) response at a 1 mm gap reflects the case where the lower plasma density than exists at the 0.5 mm gap is offset with a longer path through the plasma. Increasing the electrode separation beyond 1 mm, and thus increasing the plasma volume (i.e., dilution of the plasma $n_e$ by expansion), yields a steadily decreasing emission response even though the plasma residence times are increased. An interesting consequence of the longer, and perhaps more uniform, plasma residence times at the longer separation distances is seen in much improved sample-to-sample precision, decreasing from 21.7% at the shortest distance to 6.5% RSD for the largest gap.

Different from the case of the electrode gap lengths, where residence time and plasma volumes are affected, changes in the carrier gas velocity might be assumed to only effect the residence times. This is in fact not the case as $T_{rot}$ values decrease appreciably (900–700 K for $N_2$) with increased carrier gas flow rate, while $T_{exc}$ and $n_e$ values show strong positive correlations.[23] Thus, a more energetic plasma in terms of spectroscopic factors is achieved at high carrier gas flow rates, while low gas rates yield higher gas kinetic temperatures ($T_{rot}$) to affect greater vaporization. As seen in Fig. 3b, it is clear that low carrier gas flow rates, yielding the longest residence times and kinetically hotter environments, provide the greatest response for the 1 mm interelectrode separation distance. Indeed, operation at flow rates $<$0.2 L $min^{-1}$ caused overheating of the hollow counter electrode; so, this value was maintained as further parameters were evaluated. Gas velocity calculations suggest that the plasma transit times range from 0.5 to 0.06 ms as the flow rate is increased. Clearly seen is a near exponential decrease in the Cu(I) responses with increasing flow rates, while at the same time, the precision of replicate experiments deteriorates. Specifically, the variability is only 9% RSD for the case of 0.1 L $min^{-1}$ flow rate, increasing to 36% RSD for the highest rate of 0.8 L $min^{-1}$. The observed response reflects the fact that higher LA gas flow rates lead to decreases in the gas kinetic temperatures as well as shorter plasma residence times. Thus, as in the case of the short interelectrode distances, higher flow rates

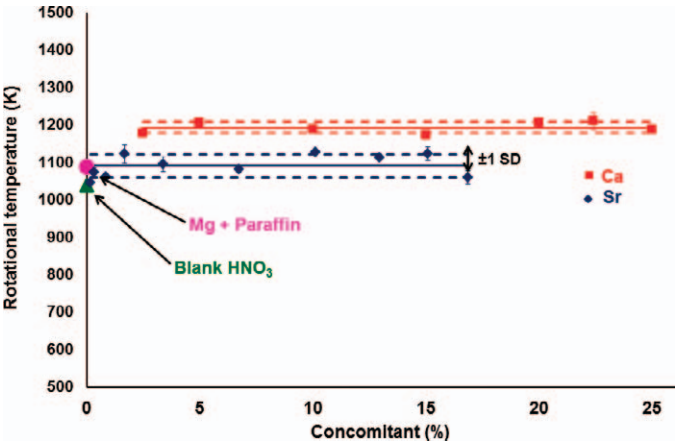


FIG. 4. $N_2$-derived rotational temperatures upon introduction of various amounts of Ca and Sr carbonates into the LS-APGD microplasma through LA of paraffin-based pellets, each doped with 3.8% (w/w) $MgCO_3$. All other parameters constant: He sheath gas flow rate = 0.2 L $min^{-1}$, solution flow rate 200 μL $min^{-1}$ (5% $HNO_3$), discharge current = 60 mA, interelectrode separation = 1.0 mm, He carrier gas flow rate = 0.2 L $min^{-1}$, 213 nm laser energy = 5 mJ, repetition rate = 10 Hz.

limit the time available for particle digestion and atomic excitation.

These studies strongly indicate that conditions that favor higher gas kinetic temperatures and longer residences time are the controlling influences on the emission response of LA-produced particulates. However, actual residence times and plasma volumes must be determined in future investigations as done by, e.g., Aeschliman et al.[29], by using high-speed digital photographs and videos. Certainly, such experimental data should be supported by detailed gas-dynamic simulations. The effect of particle residence time in the plasma on S/Ns, emission response, and sensitivity must be addressed in the future to develop a better fundamental understanding of the LS-APGD as a secondary excitation–ionization source. In this regard, the role of the sheath–cooling gas flow is also expected to be a determining factor in analytical performance.

**Robustness of Liquid Sampling–Atmospheric Pressure Glow Discharge Microplasma upon Introduction of LA-Generated Particle Aerosols.** One of the fundamental characteristics to be ascertained about any spectrochemical device is its immunity to sample–matrix-induced perturbations, i.e., its robustness. In the field of atomic spectroscopy, matrix effects can lead to pronounced quantitative errors based on several experimental factors impacting the sample introduction efficiencies, the ability to effectively vaporize the material, and changes in the excitation–ionization characteristics. There can be confusion when referring to "robustness" in the field of atomic spectrometry; robustness as an adjective describing the immunity to perturbations and the "robustness factor" that is a derived quantity that reflects the likely immunity to changes and the extent of excitation of ionic and atomic transitions.[30,31] The robustness of a source can be assessed through the measurement of certain quantities such as excitation, rotation, and ionization temperatures or perhaps electron number densities upon introduction of different sample matrices. The robustness factor is usually assessed by means of measuring specific ion-to-atom line ratios (e.g., Mg(II):Mg(I) and/or Zn(II):Zn(I)). The utility of using Mg II:Mg I ratios to assess excitation–ionization conditions in terms of the robustness factor was described in detail by Mermet.[30,31] In this case, the ratio of measured (raw) intensities of the Mg(II) 279.5 nm and the Mg(I) 285.2 nm transitions is used. In simple terms, high robustness values reflect conditions for efficient ionization, which should equate to lower susceptibility to matrix effects. In practice, one ultimately desires robustness values that do not change with conditions, indicative of low levels of plasma perturbation.

As a general approach to assessing the robustness of a spectrochemical source, plasma temperatures and ion-to-atom emission ratios are evaluated upon introduction of easily ionized elements (EIEs),[32–34] as these species tend to lead to atomization–excitation–ionization process disruption. Therefore, introducing elements such as Sr and Ca at varying concentrations can provide greater understanding of plasma robustness.[23] To investigate spectroscopic matrix effects and determine the robustness of the LS-APGD secondary excitation source for LA-generated particle aerosols, plasma rotational temperatures and Mg(II):Mg(I) ratios were monitored following the ablation of alkaline earth metal carbonate-doped paraffin pellets. Previous studies had shown that neither the excitation or rotational temperatures, electron number densities, nor the robustness factors were changed upon the introduction of LA-produced particles from Mg metal shards compacted in paraffin.[23] By the same token, microplasma excitation temperatures were unaffected by the introduction of a wide variety of concomitant elements in the liquid phase sampling using the LS-APGD.[23] Therefore, as rotational temperatures should reflect thermal loading of the plasma due to the introduction of refractory particulates, this, along with the robustness factor, was studied here. The ablated pellets contained various amounts of Ca and Sr (Table I) as EIE elements, while the Mg content was held constant. Laser ablation was accomplished using the 213 nm laser ablation system, applying LA-optimized LS-APGD instrumental parameters (Table II).

Plasma rotational temperatures were determined by fitting the N molecular bands as done in previous LS-APGD measurements.[23] As can be seen in Fig. 4, a temperature increase of ~50 K was observed upon ablation of the $MgCO_3$–paraffin (3.8% (w/w)) pellet in comparison to the steady introduction of $HNO_3$ as the electrolytic solution. Based on the reproducibility of these experiments, this difference is statistically significant. As such, the introduction of these predominately organic particles (vaporized paraffin most likely condensing with the inorganic additives in the gas phase) has no effect on the plasma energetics. Addition of $SrCO_3$ powder into the paraffin matrix yields no appreciable changes to the measured $T_{rot}$ values. In fact, the percentage of carbonate added has no effect on the measured temperatures. This is a significant finding as at the highest of the Sr loadings, metal carbonates make up ~20% of the sample by weight, a significant change in matrix. Addition of $CaCO_3$ as the concomitant element is seen to increase the $T_{rot}$ values by ~100 K.

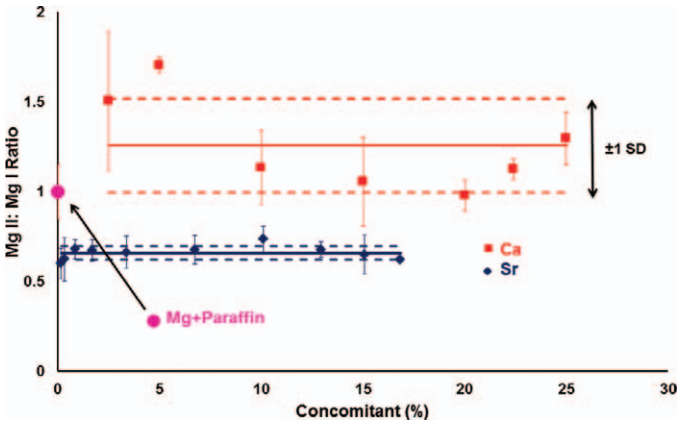


FIG. 5. Response of Mg(II) : Mg(I) (279.5 nm:285.2 nm) line ratios upon introduction of various amounts of Ca and Sr carbonates into the LS-APGD microplasma through LA of paraffin-based pellets, each doped with 3.8% (w/w) $MgCO_3$. All other parameters constant: He sheath gas flow rate = 0.2 L $min^{-1}$, solution flow rate 200 μL $min^{-1}$ (5% $HNO_3$), discharge current = 60 mA, interelectrode separation = 1.0 mm, He carrier gas flow rate = 0.2 L $min^{-1}$, 213 nm laser energy = 5 mJ, repetition rate = 10 Hz.

Here again, there is no specific influence of the actual Ca weight percentage across values of ~1.2–25%, by weight (~30% total inorganic composition). While the influence is indeed minimal, the slight increase with the introduction of Ca was also observed with the introduction of the Ca concomitant in a previous publication.[23] Those studies compared a range of physical, chemical, and spectroscopic differences among concomitants (including Ca and Sr) and could find no specific correlations; except that overall the changes were fairly minimal. It has been previously proposed by Kitagawa and Takeuchi,[34] while studying a microwave-induced plasma, that the increase of EIEs into the source would increase the overall collision rates in the plasma, resulting in an increased the plasma temperatures. The respective rotational temperatures in Fig. 3 are consistent with previous LS-APGD microplasma studies, wherein Mg was introduced in the electrolytic solution phase, with the average values across a very wide range of plasma parameters being ~1100 K.[23] Previous work wherein these elements were added in to the electrolytic flow (500 μg $mL^{-1}$) of the LS-APGD resulted in differences in excitation and ionization temperatures of <10%, relative.[23] Even though two distinct temperature ranges are observed after the ablation of Sr- and Ca-containing pellets, the plasma is considered as relatively robust as the relative difference between the two elements is only ~9%.

The response of the measured Mg(II) : Mg(I) ratios as a function of the composition of the ablated samples is depicted in Fig. 5 for the cases of the Sr and Ca concomitants. The corresponding value (1.0) for the Mg-only doped paraffin is included as a reference point. Similar to what was seen for the case of the rotational temperatures discussed above, the average value for the Ca-doped samples increases, while the Sr-doped samples lowered the robustness factor values. These relative values are also consistent with what was seen for the liquid phase introduction of these elements into the microplasma.[23] True for both concomitant elements is the fact that the robustness factor values do not change to an appreciable extent as the dopant levels are increased to values above 16 and 25% for Sr and Ca, respectively. The variability seen here reflects the case that introduction of Ca (Mg(II) :Mg( I) = 1.25 ± 0.25) leads to greater plasma instability than for Sr (Mg(II) :Mg( I) = 0.66 ± 0.04). Here, we again make the distinction between the absolute value of the robustness factor, which are very much higher for the inductively coupled plasma (ICP) (~13) than the LS-APGD,[35] and the fact that those values are very consistent upon matrix loading. Thus, while the microplasma is relatively weak in terms of the production of excited state ions, it is indeed *robust* in terms of its immunity to matrix effects. In fact, the raw Mg(II) and Mg(I) intensities showed only slight decreases under increased Ca concentrations, with no appreciable trends seen upon Sr addition. The ionic lines are more affected (~15% lower) in regards to increased $CaCO_3$ loading when compared to the atomic lines. This is also reflected in the greater variability in the robustness factor values for the Ca-doped pellets. It is suggested that in the case of introducing large amounts of concomitants into the plasma, more energy is dedicated to the vaporization of particles, and thus less energy is available for the production of excited state analyte ions.

## CONCLUSIONS

For LS-APGD to be a viable candidate as a secondary excitation for the analysis of LA-generated particles, and perhaps an alternative to inductively coupled plasma optical emission spectrometry, the factors that affect vaporization and excitation processes must be well characterized and understood. In this work, a homogeneous brass alloy was used to assess the roles of the discharge current, electrode gap, and particle carrier gas flow rates on Cu(I) signal responses. As expected, atomic emission intensities increase with discharge current, while the electrode separation and gas flow rates generate responses that reflect trade-offs affecting residence time within the plasma volume, and, ultimately, the vaporization processes. The influence of instrumental parameters (i.e., LA carrier gas flow rate, electrode gap, and GD current) on the emission response demonstrated the necessity of a thorough investigation and optimization. Low LA carrier gas flow rates (i.e., 0.1 L $min^{-1}$) and large electrode distances are suggested to be favorable in terms of longer plasma residence times. However, in case of larger electrode gap distances and resulting larger plasma volumes, less energy is available per cubic millimeter for vaporization–excitation processes, which results in an overall loss of emission response. The resulting trends were the same for 1064 and 213 nm ablation.

Ablation of metal carbonate-doped paraffin pellets using 213 nm irradiation was used to evaluate the robustness of the plasma in terms of potential changes in rotational temperatures and robustness factor values. $MgCO_3$ was doped at a constant weight percentage, with Ca and Sr carbonates added to values of ~25 and 17% (w/w), respectively. In both instances, ablation of Ca-doped particles resulted in slight increases in the metric

values, with Sr-doped samples slightly depressing the values. Both of these findings are consistent with the introduction of these elements into the solution flow of the LS-APGD. The lack of appreciable matrix effects upon introduction of the relatively large nanosecond-pulse LA particulates is believed to be a result of the high power densities ($>10$ W mm$^{-3}$) affected by the microplasma design, relatively high electron number densities ($10^{15}$–$10^{16}$ cm$^{-3}$), and relatively long residence times given the plasma size.

The results presented here are quite encouraging in terms of the implementation of the LS-APGD microplasma as a secondary excitation source for particle populations generated by laser ablation. Many fundamental questions remain to be answered that may lead to better quantitative performance. For example, understanding trade-offs between the kinetics (e.g., plasma residence time) and thermodynamics (e.g., gas kinetic temperatures) of the particle vaporization process. The determination of actual plasma residence times must be addressed in future investigations, using, e.g., a camera for high-speed photographic and video studies. Likewise the roles of the composition and velocity of the sheath–cooling gas must be taken into account. Other fundamental questions include the potential extent of elemental fractional occurring as particles vaporize (separate from that possibly occurring in the LA process). While the focus of this work was on the role of discharge operation parameters on plasma processes, the same sorts of studies must be undertaken in terms of analytical performance (e.g., calibration quality and LODs). Ultimately, detailed comparisons with LIBS and LA-ICP-OES are needed to determine the analytical utility of the method. Overall, the results of these and previous studies suggest that the LA-LS-APGD-OES system has promise for use in miniaturized, field-deployable instrumentation for performing rapid, in situ analyses.


#### ACKNOWLEDGMENTS

This work was supported by the Director, Office of Science, Office of Basic Energy Sciences, Chemical Sciences, Geosciences, and Biosciences Division, and the Deputy Administrator for Defense Nuclear Nonproliferation, Assistant Deputy Administrator for Nonproliferation Research and Development of the U.S. Department of Energy under contract DE-AC02-05CH11231.



1. A. Rios, A. Escarpa, B. Simonet. Miniaturization of Analytical Systems: Principles, Designs and Applications. Chichester, UK: John Wiley and Sons, 2009.
2. G. McMahon. Analytical Instrumentation: a Guide to Laboratory, Portable and Miniaturized Instruments. Chichester, UK: John Wiley and Sons, 2007.
3. R. Russo, X. Mao, H. Liu, J. Gonzalez, S. Mao. "Laser Ablation in Analytical Chemistry—A Review". Talanta. 2002. 57(3): 425-451.
4. R.E. Russo, X. Mao, J.J. Gonzalex, V. Zorba, J. Yoo. "Laser Ablation in Analytical Chemistry". Anal. Chem. 2013. 85(13): 6162-6177.
5. K. Niemax. "Laser Ablation – Reflections on a Very Complex Technique for Solid Sampling". Fresenius J. Anal. Chem. 2001. 370(4): 332-340.
6. R.E. Russo, X. Mao, J.H. Yoo, J. Gonzalez, P.S. Jagdish, N.T. Surya. Laser Ablation, Laser Induced Breakdown Spectroscopy. Amsterdam, The Netherlands: Elsevier, 2007.
7. B. Hattendorf, C. Latkoczy, D. Günther. "Laser Ablation-ICPMS". Anal. Chem. 2003. 75(15): 341A-347A.
8. J. Gonzalez, C. Liu, S. Wen, X. Mao, R. Russo. "Metal Particles Produced by Laser Ablation for ICP-MS Measurements". Talanta. 2007. 73(3): 567-576.
9. R. Wiens, S. Maurice, B. Barraclough, M. Saccoccio, W. Barkley, J.F. Bell III, S. Bender, J. Bernardin, D. Blaney, J. Blank, M. Bouyé, N. Bridges, N. Bultman, P. Caïs, R. Clanton, B. Clark, S. Clegg, A. Cousin, D. Cremers, A. Cros, L. DeFlores, D. Delapp, R. Dingler, C. D'Uston, M.D. Dyar, T. Elliott, D. Enemark, C. Fabre, M. Flores, O. Forni, O. Gasnault, T. Hale, C. Hays, K. Herkenhoff, E. Kan, L. Kirkland, D. Kouach, D. Landis, Y. Langevin, N. Lanza, F. LaRocca, J. Lasue, J. Latino, D. Limonadi, C. Lindensmith, C. Little, N. Mangold, G. Manhes, P. Mauchien, C. McKay, E. Miller, J. Mooney, R. Morris, L. Morrison, T. Nelson, H. Newsom, A. Ollila, M. Ott, L. Pares, R. Perez, F. Poitrasson, C. Provost, J. Reiter, T. Roberts, F. Romero, V. Sautter, S. Salazar, J. Simmonds, R. Stiglich, S. Storms, N. Striebig, J. Thocaven, T. Trujillo, M. Ulibarri, D. Vaniman, N. Warner, R. Waterbury, R. Whitaker, J. Witt, B. Wong-Swanson. "The ChemCam Instrument Suite on the Mars Science Laboratory (MSL) Rover: Body Unit and Combined System Tests". Space Sci. Rev. 2012. 170(1-4): 167-227.
10. S. Guirado, F. Fortes, V. Lazic, J. Laserna. "Chemical Analysis of Archeological Materials in Submarine Environments Using Laser-Induced Breakdown Spectroscopy. On-Site Trials in the Mediterranean Sea". Spectrochim. Acta, Part B. 2012. 74-75: 137-143.
11. V. Lazic, J. Laserna, S. Jovicevic. "Insights in the Laser-Induced Breakdown Spectroscopy Signal Generation Underwater Using Dual Pulse Excitation — Part I: Vapor Bubble, Shockwaves and Plasma". Spectrochim. Acta, Part B. 2013. 82: 42-49.
12. J. Gonzalez, C. Liu, S. Wen, X. Mao, R. Russo. "Glass Particles Produced by Laser Ablation for ICP-MS Measurements". Talanta. 2007. 73(3): 577-582.
13. K. Li, W. Zhou, Q. Shen, Z. Ren, B. Peng. "Laser Ablation Assisted Spark Induced Breakdown Spectroscopy on Soil Samples". J. Anal. At. Spectrom. 2010. 25(9): 1475-1481.
14. Y. Iida. "Laser Vaporization of Solid Samples into a Hollow-Cathode Discharge for Atomic Emission Spectrometry". Spectrochim. Acta, Part B. 1990. 45(4-5): 427-438.
15. K. Tereszchuk, J. Vadillo, J. Laserna. "Energy Assistance in Laser Induced Plasma Spectrometry (LIPS) by a Synchronized Microsecond-Pulsed Glow Discharge Secondary Excitation". J. Anal. At. Spectrom. 2007. 22(2): 183-186.
16. K. Becker, K. Schoenbach, J. Eden. "Microplasmas and Applications". J. Phys. D Appl. Phys. 2006. 39(3): R55-R70.
17. N. Jakubowski, R. Dorka, E. Steers, A. Tempez. "Trends in Glow Discharge Spectroscopy". J. Anal. At. Spectrom. 2007. 22(7): 722-735.
18. M.R. Webb, G.M. Hieftje. "Spectrochemical Analysis by Using Discharge Devices with Solution Electrodes". Anal. Chem. 2009. 81(3): 862-867.
19. X. Yuan, J. Tang, Y. Duan. "Microplasma Technology and Its Applications in Analytical Chemistry". Appl. Spectrosc. Rev. 2011. 46(7): 581-605.
20. P. Jamroz, K. Greda, P. Pohl. "Development of Direct-Current, Atmospheric-Pressure, Glow Discharges Generated in Contact with Flowing Electrolyte Solutions for Elemental Analysis by Optical Emission Spectrometry". Trends Anal. Chem. 2012. 41: 105-121.
21. A.J. Carado, C.D. Quarles, Jr., A.M. Duffin, C.J. Barinaga, R.E. Russo, R.K. Marcus, D.W. Koppenaal. "Femtosecond Laser Ablation Particle Introduction to a Liquid Sampling-Atmospheric Pressure Glow Discharge Ionization Source". J. Anal. At. Spectrom. 2012. 27(3): 385-389.
22. C. Quarles, J. Gonzalez, I. Choi, J. Ruiz, X. Mao, R. Marcus, R. Russo. "Liquid Sampling-Atmospheric Pressure Glow Discharge Optical Emission Spectroscopy Detection of Laser Ablation Produced Particles: A Feasibility Study". Spectrochim. Acta, Part B. 2012. 76: 190-196.
23. B.T. Manard, J. Gonzalez, A. Sarkar, M. Dong, J. Chirinos, X. Mao, R.E. Russo, R.K. Marcus. "Liquid Sampling-Atmospheric Pressure Glow Discharge as a Secondary Excitation Source: Assessment of Plasma Characteristics". Spectrochim. Acta, Part B. 2014. 94-95: 39-47.
24. R.K. Marcus, W.C. Davis. "An Atmospheric Pressure Glow Discharge Optical Emission Source for the Direct Sampling of Liquid Media". Anal. Chem. 2001. 73(13): 2903-2910.
25. W.C. Davis, R.K. Marcus. "An Atmospheric Pressure Glow Discharge Optical Emission Source for the Direct Sampling of Liquid Media". J. Anal. At. Spectrom. 2001. 16(9): 931-937.
26. D. Fang, R.K. Marcus. "Fundamental Plasma Processes". In: R.K. Marcus, editor. Glow Discharge Spectroscopies. New York: Plenum Press, 1993. Pp. 17-66.

27. R. Savage, G. Hieftje. ‘‘Vaporization and Ionization Interferences in a Miniature Inductively Coupled Plasma’’. Anal. Chem. 1980. 52(8): 1267-1272.
28. I. Novotny, J. Farinas, J. Wan, E. Poussel, J. Mermet. ‘‘Effect of Power and Carrier Gas Flow Rate on the Tolerance to Water Loading in Inductively Coupled Plasma Atomic Emission Spectrometry’’. Spectrochim. Acta, Part B. 1996. 51(12): 1517-1526.
29. D. Aeschliman, S. Bajic, D. Baldwin, R. Houk. ‘‘High-Speed Digital Photographic Study of an Inductively Coupled Plasma During Laser Ablation: Comparison of Dried Solution Aerosols from a Microconcentric Nebulizer and Solid Particles from Laser Ablation’’. J. Anal. At. Spectrom. 2003. 18(9): 1008-1014.
30. J. Mermet. ‘‘Use of Magnesium as a Test Element for Inductively Coupled Plasma Atomic Emission Spectrometry Diagnostics’’. Anal. Chim. Acta. 1991. 250: 85-94.
31. J. Mermet. ‘‘Revisitation of the Matrix Effects in Inductively Coupled Plasma Atomic Emission Spectrometry: The Key Role of the Spray Chamber—Invited Lecture’’. J. Anal. At. Spectrom. 1998. 13(5): 419-422.
32. G. Chan, W. Chan, X. Mao, R. Russo. ‘‘Investigation of Matrix Effects in Inductively Coupled Plasma-Atomic Emission Spectroscopy Using Laser Ablation and Solution Nebulization—Effect of Second Ionization Potential’’. Spectrochim. Acta, Part B. 2001. 56(1): 77-92.
33. G. Chan, W. Chan, X. Mao, R. Russo. ‘‘Investigation of Matrix Effect on Dry Inductively Coupled Plasma Conditions Using Laser Ablation Sampling’’. Spectrochim. Acta, Part B. 2000. 55(3): 221-235.
34. K. Kitagawa, T. Takeuchi. ‘‘Spectroscopic Studies of Microwave-Excited Plasma’’. Anal. Chim. Acta. 1972. 60(2): 309-318.
35. G. Chan, G. Hieftje. ‘‘Investigation of Plasma-Related Matrix Effects in Inductively Coupled Plasma-Atomic Emission Spectrometry Caused by Matrices with Low Second Ionization Potentials—Identification of the Secondary Factor’’. Spectrochim. Acta, Part B. 2006. 61(6): 642-659.